

How does homophily shape the topology of a dynamic network?Xiang Li ¹, Mauro Mobilia ¹, Alastair M. Rucklidge ¹ and R. K. P. Zia ^{2,3,4}¹*Department of Applied Mathematics, School of Mathematics, University of Leeds, Leeds LS2 9JT, United Kingdom*²*Center for Soft Matter and Biological Physics, Department of Physics,**Virginia Polytechnic Institute & State University, Blacksburg, Virginia 24061, USA*³*Department of Physics & Astronomy, University of North Carolina at Asheville, Asheville, North Carolina 28804, USA*⁴*Physics Department, University of Houston, Houston, Texas 77204, USA*

(Received 30 June 2020; revised 30 July 2021; accepted 20 September 2021; published 19 October 2021)

We consider a dynamic network of individuals that may hold one of two different opinions in a two-party society. As a dynamical model, agents can endlessly create and delete links to satisfy a preferred degree, and the network is shaped by *homophily*, a form of social interaction. Characterized by the parameter $J \in [-1, 1]$, the latter plays a role similar to Ising spins: agents create links to others of the same opinion with probability $(1 + J)/2$ and delete them with probability $(1 - J)/2$. Using Monte Carlo simulations and mean-field theory, we focus on the network structure in the steady state. We study the effects of J on degree distributions and the fraction of cross-party links. While the extreme cases of homophily or heterophily ($J = \pm 1$) are easily understood to result in complete polarization or anti-polarization, intermediate values of J lead to interesting features of the network. Our model exhibits the intriguing feature of an “overwhelming transition” occurring when communities of different sizes are subject to sufficient heterophily: agents of the minority group are oversubscribed and their average degree greatly exceeds that of the majority group. In addition, we introduce an original measure of polarization which displays distinct advantages over the commonly used average edge homogeneity.

DOI: [10.1103/PhysRevE.104.044311](https://doi.org/10.1103/PhysRevE.104.044311)**I. INTRODUCTION**

Simple individual-based models have been commonly used to describe emergent social phenomena [1]. Statistical physics models have proven particularly useful to characterize collective behaviors of interacting populations [2–5]. In the past two decades, there have been numerous advances in understanding the properties of these interdisciplinary models notably on social networks [6–8]. An important line of research has focused on dynamical processes on networks, particularly on opinion dynamics [2] and evolutionary processes [9]. In this context, the dynamics of paradigmatic statistical physics models have been studied on complex networks whose structure is random but static; see, e.g., Refs. [10–17]. In other models, collective phenomena emerge from the interactions between agents whose links evolve while the states of the nodes (e.g., representing agents’ “opinions”) remain static. This is for instance the case when individuals are more likely to bond and create links as they are more like-minded, see, e.g., Refs. [18–20], a form of social interaction referred to as “homophily” or “assortative mixing” [8,21–25].

Social networks are comprised of individuals with a variety of attributes, such as opinion, race, age, educational background, or gender [26–28]. The level of homophily in a society thus reflects the tendency of individuals to establish ties with those having similar attributes to theirs rather than with others [21,27,29,30]. This phenomenon, reminiscent of filter bubbles and echo chambers, is commonly seen in political parties [31–37]. Similarly, *heterophily* refers to

the tendency to establish links between agents with different attributes (or dissenting “opinions”) [38–41]. Studying how homophily and/or heterophily influence the network structure has gained importance in both sociological [22,23,25,27–30,42] and physics-oriented literature [19,43–48]. In this context, homophily often features in so-called nodal attribute models [19,43,49] and growing networks like those of Refs. [42,44,46,50], where it is generally modeled by means of a biased probability of adding a link or by rewiring an edge. Homophilic interactions are often considered together with the process of structural balance [51], which aims at eliminating tensions between a set of three connected agents (triad) by the principle of “triad closure” [47,49]. By combining homophilic edge weighting and triad closure, it was recently shown that a transition to a state of global cooperation can occur [49]. In Ref. [47], it is shown that homophilic rewiring combined with triad closure leads to “homophily amplification,” a phenomenon in which agents within a same group are likely to interact and establish further connections. Furthermore, voter-like models evolving on a network whose links are dynamically updated according to a homophilic rewiring process [52–58] are characterized by a continuous phase transition yielding the fragmentation [54,55], or fission [57], of the network into disconnected groups holding the same opinion.

Here, we consider an evolving network model in which links fluctuate continuously as the result of the homophilic or heterophilic interactions between individuals of two communities (e.g., political parties). Contrary to most previous

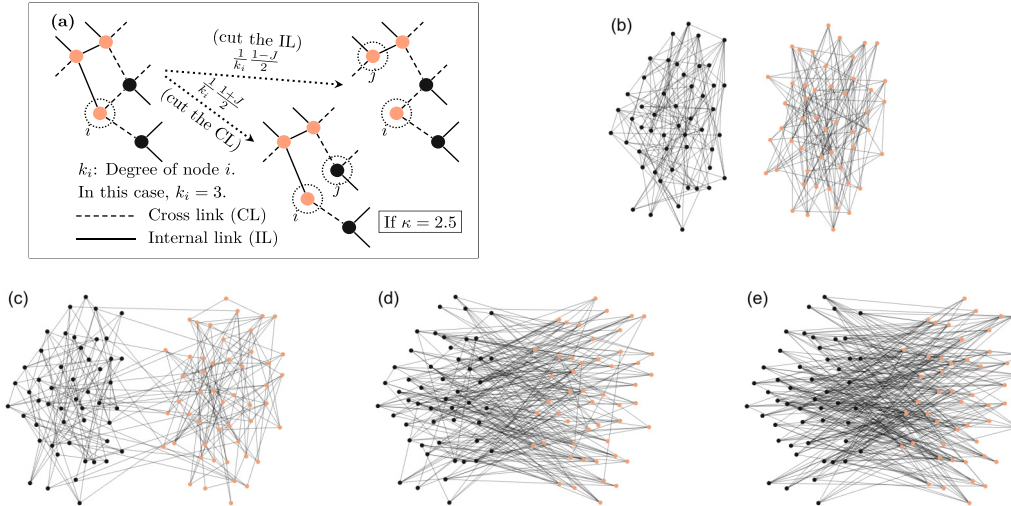


FIG. 1. (a) Illustration of the link update rule with preferred degree $\kappa = 2.5$ and homophily parameter J . Here, a node i of degree $k_i = 3 > \kappa$ first selects one of its neighbors uniformly (node j); in the next time step, the link ij is cut with probability $(1 - J)/2$ if $\sigma_i = \sigma_j$ [ij is an internal link (IL)], and with probability $(1 + J)/2$ if $\sigma_i = -\sigma_j$ (ij is a cross link, CL). CLs and ILs are necessarily cut only when $J = 1$ (extreme homophily) and $J = -1$ (extreme heterophily), respectively. Similarly, if $k_i < \kappa$ (not shown here), then in the next time step an IL ij is created with probability $(1 + J)/2$ with a new neighbor j of the same opinion ($\sigma_i = \sigma_j$), while a CL ij is created with probability $(1 - J)/2$ with a new dissenting neighbor ($\sigma_i \neq \sigma_j$). (b)–(e) Different polarization scenarios after 100 Monte Carlo steps (MCS, 1 MCS = N update steps) starting with an empty graph (i.e., no links). Here, light and dark dots are voters (or nodes) i and i' holding opinion -1 ($\sigma_i = -1$) and $+1$ ($\sigma_{i'} = +1$), respectively. Here, $N = 100$, $m = 0$ (communities of same size: $N_+ = N_- = 50$), $\kappa = 4.5$ in panels (b)–(e), and (b) $J = 1$, (c) $J = 0.5$, (d) $J = -0.5$, (e) $J = -1$; see text.

works on networks with homophily, the dynamics shaped by homophily here follows an evolutionary process characterized by the continuous creation and deletion of edges, with an endlessly fluctuating number of links. More specifically, we adopt the language of opinion dynamics and consider an individual-based network model where agents hold one of two different opinions [59–62], and form dynamical links to satisfy a prescribed preferred degree [63–65]. The model dynamics can therefore be thought of as a “birth-death process” for links, with transition rates depending on a homophily parameter characterizing the interactions between nodes. As other preferred degree networks (PDNs) [63–65], our model is characterized by a nontrivial out-of-equilibrium stationary state. By combining analytical means and simulations, we determine how the homophily shapes the long-time network structure, typically characterized by the degree distributions and the fraction of cross-party links. We also quantify the extent of division between the communities by computing the network’s polarization. This allows us to show that our model shares some features found in earlier works, such as a fragmentation (or fission) transition under extreme homophily [see Fig. 1(a) and below]. More importantly, we also show that our model exhibits intriguing features such as an “overwhelming transition” occurring when communities of different sizes are subject to sufficient heterophily: agents of the minority group are oversubscribed and their average degree greatly exceeds that of the majority group.

The plan of the paper is as follows: the general formulation of the model based on PDN dynamics with homophilic interactions is introduced in the next section. In Sec. III, by combining a mean-field analysis and Monte Carlo simulations, we present a thorough study of the model’s properties

when both parties are of the same size: the fractions of cross-party links and of agents adding links is obtained in Sec. III A, while Sec. III B is dedicated to the network’s degree distributions. In Sec. IV, we consider the general case of communities of different sizes: in Sec. IV A, we show that under sufficient heterophily the network consists only of agents deleting nodes; while the model’s polarization is discussed in Sec. IV B. In Sec. V, we introduce a quantity that efficiently measures the network’s polarization. The final section is dedicated to a discussion of our results and to our conclusions.

II. MODEL FORMULATION AND GENERAL PROPERTIES

Our model is an undirected dynamical network consisting of N nodes (or agents/voters) that are of two types: a fraction n_+ of them is in state $+1$, while the remaining fraction $n_- = 1 - n_+$ is in state -1 . Hence, the population consists of number $N_\pm = Nn_\pm$ agents holding opinion ± 1 . In the language of opinion dynamics, each node i is a “voter” whose opinion is the binary random variable $\sigma_i \in \{-1, +1\}$, i.e., each voter belongs to either party -1 or $+1$. For simplicity, here $\{\sigma\}$ are quenched variables, i.e., voters are “zealots” [59,61,62,66] (see also Refs. [67–70]). The average opinion, often referred to as “magnetization,” across the network is $m = \frac{1}{N} \sum_{i=1}^N \sigma_i = n_+ - n_-$, so that $n_\pm = \frac{1}{2}(1 \pm m)$. Hence, when the magnetization vanishes, $m = 0$, each party is a group of the same size, that is $N_+ = N_-$.

According to the PDN dynamics, every node is assigned a preferred degree κ , a value each agent attempts to achieve by cutting or adding links [71]. The update rules of the model, illustrated in Fig. 1(a), are thus as follows: at each update step, an agent i of degree k_i is chosen randomly and

(1) if $k_i > \kappa$, then the node i chooses a neighbor j with uniform probability among all its neighbors, and then either (i) the ij link is cut with the probability $\frac{1}{2}(1 - J\sigma_i\sigma_j)$, or (ii) the ij link remains unchanged.

(2) if $k_i < \kappa$, then the node i chooses uniformly a random node j to which it is not already connected, and then either (i) the new link ij is added with probability $\frac{1}{2}(1 + J\sigma_i\sigma_j)$, or (ii) i and j remain unconnected.

Nodes with degrees greater than or less than κ are referred to as *cutters* and *adders*, respectively. We always take κ to be a *half integer*, with $1 \ll \kappa \ll N$ [63,65]. This guarantees that the network is always dynamic, with an endlessly fluctuating number of links, and each agent's neighborhood is a small subset of the population. Here, J is our homophily control parameter, with $-1 \leq J \leq 1$.

A distinctive feature of this PDN with homophily is its "evolutionary dynamics" shaped by homophily: links are continuously created and removed, as in a birth-death process, with rates capturing the homophilic ($J > 0$) or heterophilic ($J < 0$) agent interactions; see Eqs. (3) and (4). As illustrated in Fig. 1(a), the probability of cutting a link between two nodes is $(1 - J)/2$ if their opinions are the same, and $(1 + J)/2$ if their opinions are opposite. It is therefore clear that $J > 0$ models homophily, as it favors the addition of *internal links* (ILs) between similar nodes, and the removal of *cross links* (CLs) between nodes of different opinions. Similarly, having $J < 0$ represents heterophily that favors the creation of CLs over ILs.

While we focus on intermediate homophily, $-1 < J < 1$, with links being continuously added and cut in an endlessly fluctuating network, a system with extreme homophily or heterophily ($J = \pm 1$) is interesting as these are the only values of J for which the addition or deletion of links occurs with probability one. In fact, nodes only add ILs if $J = 1$ (CLs if $J = -1$), and the network settles in a nontrivial static configuration when every node has $k > \kappa$ and no adders are left.

This simple model is out of thermal equilibrium, as it violates detailed balance, and its stationary properties are thus expected to be nontrivial [63], as illustrated by Figs. 1(b)–1(e). Our goal is to understand how homophily shapes the properties of the steady-state network by focusing on the total degree distributions, the fractions of CLs and adders in the stationary state of the network. The total numbers of CLs and ILs are denoted by L_\times and L_\circ respectively. We can also write $L_\times = L_{+-} = L_{-+}$ and $L_\circ = L_{++} + L_{--}$, where $L_{\sigma\sigma'}$ is the number of links between communities holding opinion σ and σ' . These quantities are time-fluctuating variables and the total number of links in the network denoted by $L = L_\times + L_\circ$ is *not* conserved [63,64]. The fraction of CLs in the network is defined as $\rho = L_\times / (L_\times + L_\circ)$. When groups of ± 1 voters are of different sizes ($m \neq 0$), we shall see that it is useful to distinguish in each community the fraction of nodes that have CLs; see Secs. IV and V.

We can gain some insight into the effect of J on the network dynamics by considering the special cases $J = \pm 1$ and $J = 0$. When $J = 1$, a node adds only ILs and cuts only CLs, which leads to the population being split into two separate groups; see Fig. 1(b). This phenomenon, sometimes termed "fission" or "fragmentation," where there are no CLs ($L_\times = 0$, $\rho = 0$), is found in models with rewiring [52,55,57,58], and

corresponds *complete polarization* of the population. When $J = -1$, each node can only add CLs and cut ILs, which eventually results in *complete antipolarization*, i.e., a bipartite graph with $L_\circ = 0$, $\rho = 1$, as in Fig. 1(e). When $J = 0$, a node adds and cuts links randomly, regardless of its neighbor's opinion, leading to a state of *no polarization*, where on average half of the nodes are adders, and the average ratio of CLs to ILs, controlled purely by phase space, is $\frac{2n_+n_-}{1-2n_+n_-}$. When $0 < J < 1$, the two communities are partly divided, with a majority of ILs ($\rho < 1/2$); see Fig. 1(c). Similarly, when $-1 < J < 0$, the network consists of a majority of CLs ($\rho > 1/2$); see Fig. 1(d). Hence, the two communities are partly divided when $-1 < J < 1$, which results in a partial polarization of the network.

A common measure of polarization, sometimes referred to as "average edge homogeneity" [36,72], is the difference between the fraction of ILs and CLs, here denoted by $\Lambda \equiv (L_\circ - L_\times)/L = 1 - 2\rho \in [-1, 1]$. When $m = 0$, Λ follows homophily closely with $\Lambda = 0, \pm 1$ when $J = 0, \pm 1$, respectively. However, as shown below, its suitability deteriorates when m deviates from zero: we find that for $m \neq 0$, the network can be "polarized" ($\Lambda > 0$) even when $J = 0$. In Sec. V, we will hence introduce an alternative measure of polarization here denoted by Π .

III. SYMMETRIC CASE, $m = 0$

In this section, we focus on the symmetric case $m = 0$ where the communities of agents holding opinion ± 1 are of the same size. This symmetry greatly simplifies the analysis: the statistical properties of both communities are the same, and there is no need to distinguish between the opinion groups. Using mean-field analysis and Monte Carlo simulations, we obtain a detailed characterization of the effect of homophily on the fractions of adders and cross-links in the networks, and on the total and joint degree distributions.

A. Fractions of adders and cross-links

The network being dynamic, the fraction of adders, here denoted by α , endlessly fluctuates. To gain some insight into its distribution, it is useful to start by considering the results of some typical Monte Carlo simulations; see Fig. 2. In all our simulations, without loss of generality, we assume that there are initially no links (e.g., mimicking a population of arriving university students establishing links) and the number of nodes N is even. When $m = 0$, the network thus consists of $N/2$ nodes of each opinion. Using a range of J , κ , and N (with $\kappa \ll N$), we let the system evolve and perform a large number of update steps, N of which correspond to one Monte Carlo step (MCS), so that in one MCS each node is picked once on average for an update move. We have noticed that after typically $\mathcal{O}(\kappa)$ MCS, the quantity α (as well as other global quantities such as ρ) reaches a well-defined steady state in which the amplitude of the fluctuations decreases as the number of nodes N increases; see Figs. 2(a) and 2(b). In fact, $p(\alpha)$, the stationary probability density of α , is well fitted by a Gaussian, as shown in Figs. 2(c) and 2(d), where $p(\alpha) = 7.887 \exp[-(\frac{\alpha-0.4208}{0.07143})^2]$ when $N = 100$ and the density is narrower when $N = 1000$, in which case

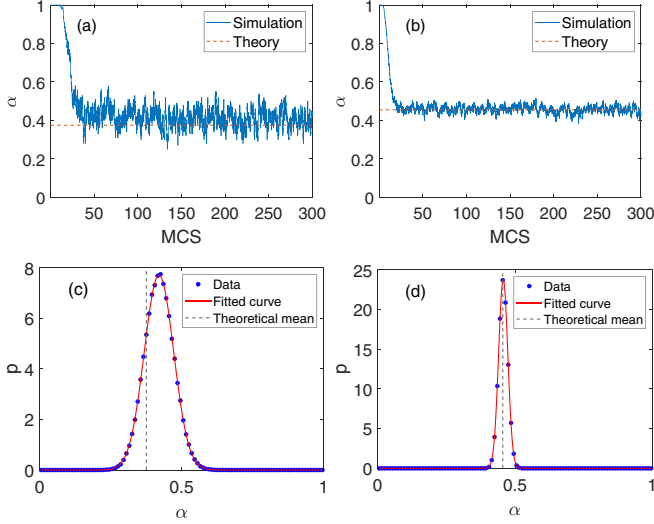


FIG. 2. Evolution and probability density of α , the fraction of adders, when $m = 0$ for different values of N , κ and J : (a), (b) typical sample paths of α as function of the time measured in the number of Monte Carlo steps (1 MCS = N update steps); (c), (d) stationary probability density $p(\alpha)$. Parameters are $(N, \kappa, J) = (100, 20.5, 0.5)$ in panels (a), (c) and $(N, \kappa, J) = (1000, 10.5, 0.3)$ in panels (b), (d). Dashed lines show the mean-field prediction $\alpha = (1 - J^2)/2$; see Eq. (2). Solid lines in panels (b), (d) are the fitted Gaussians referred to in the text. Simulation data in panels (c), (d) are obtained between 100 MCS and 5000 MCS, sampled at the end of update steps of each MCS. Data are sampled similarly in the following figures.

$p(\alpha) = 23.97 \exp[-(\frac{\alpha - 0.4565}{0.02348})^2]$. We have obtained similar results for ρ : the fraction of CLs also attains stationarity after $\mathcal{O}(\kappa)$ MCS. Throughout, with κ 's ranging from 4.5 to 70.5, we have run simulations for at least ten times longer than the time $\mathcal{O}(\kappa)$ necessary to reach stationarity. We then collected data in the steady state for various lengths of time. In our simulations, we have thus found that α and ρ approach a steady state in which samples separated by one MCS are essentially uncorrelated, where fluctuations scale as $1/\sqrt{N}$, and the total number of links L is of order $\mathcal{O}(N\kappa)$. While L , L_{\times} , L_{\odot} are time-dependent quantities, they fluctuate around their stationary values $\langle L \rangle$, $\langle L_{\times} \rangle$, $\langle L_{\odot} \rangle$. In what follows, for notational simplicity, L , L_{\times} , L_{\odot} quantities will refer to their stationary values. Similarly, in Sec. V, $L_{\pm\pm}$ denotes $\langle L_{\pm\pm} \rangle$.

The simulation results of Fig. 2 strongly support a mean-field analysis in which the fraction of adders and CLs would simply be described by their stationary average values. When $-1 < J < 1$, we obtain mean-field predictions for these values, simply referred to as α and ρ , by balancing the tendency for L_{\times} and L_{\odot} to increase and decrease in the stationary state. For L_{\times} to increase, an adder, picked with probability α , must interact with a nonneighbor of different opinion with probability $1/2$ (since $n_{\pm} = 1/2$), adding a link with probability $(1 - J)/2$. Similarly, for L_{\times} to decrease, a cutter, picked with probability $1 - \alpha$, must interact with one of its dissenting neighbors (with probability ρ), cutting the link with probability $(1 + J)/2$. Balancing these contributions leads to $\alpha(1 - J) = 2(1 - \alpha)(1 + J)\rho$. Similar considerations for the

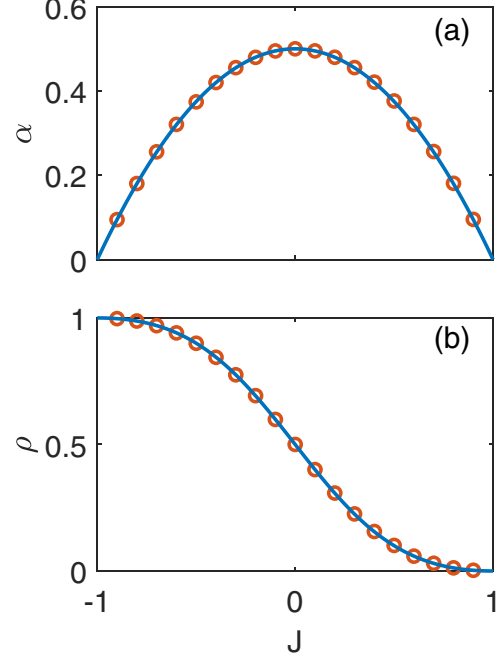


FIG. 3. Fractions of adders α and of CLs ρ in the steady state as functions of the homophily parameter for $N = 1000$, $\kappa = 4.5$, and $m = 0$. (a) α vs J : solid line is from Eq. (1), symbols are obtained by averaging simulation data collected between 100 MCS and 5000 MCS. (b) Same for ρ vs J : solid line is from Eq. (2).

changes in L_{\odot} lead to the following additional equation $\alpha(1 + J) = 2(1 - \alpha)(1 - J)(1 - \rho)$. Solving the balance equations for L_{\times} and L_{\odot} yields the mean-field predictions

$$\alpha = \frac{1}{2}(1 - J^2), \quad (1)$$

$$\rho = \frac{1}{2} - \frac{J}{1 + J^2}. \quad (2)$$

Results reported in Figs. 2 and 3 show that when $1 \ll \kappa \ll N$, the mean-field predictions for α and ρ are in excellent agreement with values obtained by averaging over simulation data, for all values of J . It is worth noting the consistency of Eqs. (1) and (2) with the consideration of the special cases above: ρ increases from 0 (complete polarization) to 1 (complete antipolarization) as the homophily parameter J decreases from 1 to -1 . At the two extremes, $J = \pm 1$, the fraction of adders α is zero. In the absence of homophily, $J = 0$, the fractions of CLs and adders are $1/2$, and there is no polarization.

B. Total and joint degree distributions

In addition to α and ρ , we are interested in determining the effect of J on the long-time network structure, characterized by its degree distributions. In this section, we investigate the total degree distribution (giving the probability for a node to have degree k in the stationary state), shown in Fig. 4(a), and the conditional degree distribution, shown in Fig. 4(b). The former can be obtained by combining the above mean-field theory with a masterlike equation obeyed by the degree distribution at time t , denoted by $p(k, t)$. If $R^a(k)$ and $R^c(k)$ are the rates at which a node of degree k adds or cuts a link, then

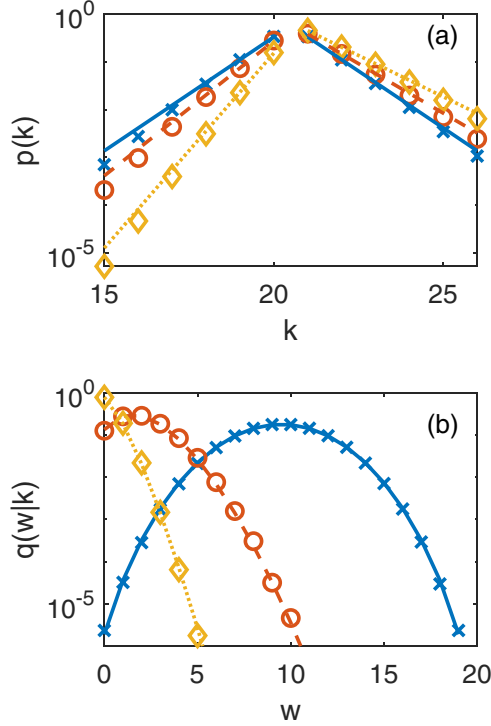


FIG. 4. (a) Total degree distribution $p(k)$ vs degree k for $N = 1000$, $\kappa = 20.5$, $m = 0$, and different values of J . Solid, dashed, and dotted lines are from Eq. (5) for different values of J . (b) Conditional distribution $q(w|k)$ vs degree $w \leq k$ for $k = 19$ and different values of J . Lines are predictions from the binomial distribution Eq. (7). Symbols represent data collected between 2000 MCS and 1 000 000 MCS. In both panels, $J = 0$ (\times , solid lines), 0.5 (\circ , dashed lines), 0.8 (\diamond , dotted lines).

$p(k, t)$ obeys

$$\frac{dp(k, t)}{dt} = R^a(k-1)p(k-1, t) + R^c(k+1)p(k+1, t) - [R^a(k) + R^c(k)]p(k, t). \quad (3)$$

Since this master equation governs a single-variate distribution, the steady state $\lim_{t \rightarrow \infty} p(k, t) = p(k)$ is obtained by balancing the probability that a node of degree k acquiring a link [with rate $R^a(k)$] with that of the node of degree $k+1$ losing a link [with rate $R^c(k+1)$], i.e., $R^a(k)p(k) = R^c(k+1)p(k+1)$. Once we determine expressions for R^a and R^c , the recursion relation and normalization condition $\sum_k p(k) = 1$ readily gives an explicit expression for $p(k)$.

Under PDN dynamics [63–65], links are added and cut from a node both actively (action by the chosen node) or passively (action by other agents). Specifically, when $k > \kappa$, a node increases its degree only passively. In one time step, an adder can be chosen with probability α and a link added with probability $\frac{1}{2} = \frac{1}{2}[\frac{1}{2}(1+J) + \frac{1}{2}(1-J)]$ (assuming that half of the nonneighbors are of the same (or different) opinion when $\kappa \ll N$). Hence, in the spirit of the mean-field approximation, this yields $R^a = \frac{\alpha}{2}$. For R^c , similar reasoning leads to the probability for cutting a link being $\chi(\rho) \equiv \frac{1}{2}(1-J)(1-\rho) + \frac{1}{2}(1+J)\rho$. Since $k > \kappa$, a node can take this action, as well as suffer a decrease passively, from the fraction $1-\alpha$

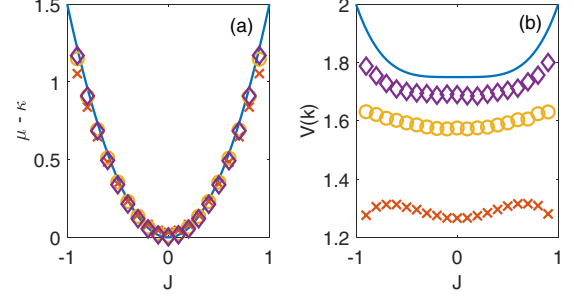


FIG. 5. (a) $\mu - \kappa$ vs J and (b) $V(k)$ vs J for $N = 1000$ and different values of κ : $\kappa = 5.5$ (\times), 20.5 (\circ), and 70.5 (\diamond). Lines are the analytical degree average and variance given by Eq. (6); markers are these quantities obtained by averaging simulation data collected between 2000 MCS and 1 000 000 MCS; see text.

of other cutters. Thus, $R^c = \chi(\rho)[1 + (1-\alpha)]$. Similar arguments can be used when $k < \kappa$, leading to $R^a = \frac{1+\alpha}{2}$ and $R^c = \chi(\rho)(1-\alpha)$. Combining these consideration, we have

$$R^a = \frac{1}{2}[H(\kappa - k) + \alpha], \quad R^c = \chi(\rho)[H(k - \kappa) + (1 - \alpha)], \quad (4)$$

where H is the Heaviside step function. Using the mean-field results Eq. (2) for ρ to rewrite χ as a function of J in Eq. (4) and solving the recursion relation, we obtain the stationary total degree distribution as the steady-state solution of Eq. (3):

$$p(k) = \begin{cases} \left(\frac{1-J^2}{3-J^2}\right)^{[\kappa]-k} & \text{for } k < \kappa, \\ \left(\frac{1+J^2}{3+J^2}\right)^{k-[\kappa]} & \text{for } k > \kappa. \end{cases} \quad (5)$$

Interestingly, $p(k)$ is an even function of J for all k 's: when $m = 0$, homophily and heterophily have the same effect on the distribution of degrees in the stationary network. This is no longer the case when $m \neq 0$; see below. We notice that Eq. (5), in accord with simulation results, predicts that $p(k)$ is symmetric with respect to κ when $J = 0$ (no polarization): in this case, we recover a Laplace distribution as in Refs. [63,65]. However, $p(k)$ is skewed as soon as there is some degree of homophily ($J \neq 0$): in Fig. 4(a), the slopes of the left branch of $\ln(p(k))$ increase from $\ln 3$ to infinity, while those of the right branch increases from $-\ln 3$ to $-\ln 2$, as $|J|$ increases from 0 to 1. Comparison with simulation results shows that these predictions Eq. (5) are in very good agreement with data over a broad range of values of J ($-1 < J < 1$) and k [Fig. 4(a)]. The deviations near the tails of the distribution are understandable, as our approximation does not account for the physical limits of $k \in [0, N]$.

With Eq. (5), we can compute the average degree $\mu = \sum_k k p(k)$ and variance $V = \sum_k (k - \mu)^2 p(k)$, whose explicit expressions read

$$\mu = \kappa + \frac{3J^2}{2} \quad \text{and} \quad V = \frac{7+J^4}{4}. \quad (6)$$

The results for μ are in good agreement with those from simulation data when $1 \ll \kappa \ll N$, and the results for V approach the theoretical prediction for large κ , as shown in Fig. 5. We notice that somewhat counterintuitively μ increases from κ monotonically with $|J|$. In other words, both homophily and heterophily increase the average degree, which

is consistent with the decrease of adders. More noteworthy is that the presence of translational invariance (in k -space) in our approximation scheme for $p(k)$, i.e., the dependence on (k, κ) is only through the difference $k - \kappa$; see Eq. (5). As a result, both $\mu - \kappa$ and V are independent of κ . In fact, $\mu - \kappa = \mathcal{O}(J^2)$ and the standard deviations from the mean degree are also of order $\mathcal{O}(J^2)$. The systematic deviations from the theoretical prediction of V in Fig. 5(b) stem from finite-size effects and decrease as κ is set further from the limits of our approximation ($1 \ll \kappa \ll N$).

To summarize, our mean-field theory, resulting in Eqs. (5) and (6), captures the essence of our model when $m = 0$ and agrees well with simulation data, with some deviations caused by some of the underpinning mean-field assumptions. In particular, we have found that the total degree distribution in the case of communities of the same size is exponential with a peak around the preferred degree κ (when $1 \ll \kappa \ll N$) with small deviations about it that increase with the level of homophily or heterophily in the population. As discussed in the next section, a totally different and more complex picture emerges when communities are of different sizes.

In addition to $p(k)$, we are also interested in how the CLs and ILs are distributed. We have thus studied the conditional distribution $q(w|k)$, giving the probability for a node of total degree k to have w CLs in the stationary state among those with total degree k . As in other network models with preferred degrees [65], we expect no bias in favor of or against a CL other than the effects of J , in such way to produce the observed value of ρ . In other words, our assumption is that, for a node with degree k , the probability of selecting one of its neighbors of the opposing opinion is just ρ . Hence, we may postulate a binomial distribution for w , the number of CLs our node has:

$$q(w|k) = \binom{k}{w} \rho^w (1 - \rho)^{k-w}. \quad (7)$$

The distribution is in excellent agreement with simulation data obtained for $q(w|k)$ with different sets of parameters, as illustrated in Fig. 4(b).

Note that when J changes sign, $J \rightarrow -J$, we have $\rho \rightarrow 1 - \rho$ and therefore $q(w|k) \rightarrow q(k - w|k)$. These “degeneracies” will be lifted once we consider communities of different sizes.

Beyond these comparisons, let us point out an interesting and sharp distinction between the total degree distribution and the conditional distribution q . The variance of the former is $\mathcal{O}(1)$. Since it is independent of extensive parameters like N and κ , the total degree distribution resembles a delta function in the large N, κ limit. By contrast, being a binomial in w , the variance of q is $\rho(1 - \rho)k$. Since the k 's of interest are $\mathcal{O}(\kappa)$, the variance here is of extensive form, a typical feature of random networks like Poisson random graphs [7,8,73], also found in rewiring models [54,55] where the mean and the variance of degrees are of the same order.

IV. ASYMMETRIC CASE $m \neq 0$

We now consider the general case where opinion groups are of different sizes, with $n_+ \neq n_-$, i.e., $m \neq 0$. In this case, each physical quantity is twofold: the fractions of adders or

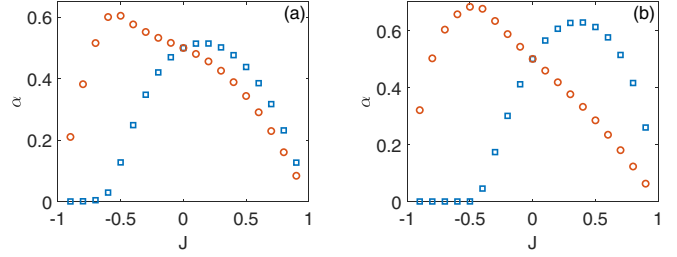


FIG. 6. Simulation results for the fraction of adders α_+ , α_- when $N = 1000$ and $\kappa = 60.5$. α_+ (blue \square) and α_- (red \circ) versus J with (a) $m = -0.2$ and (b) $m = -0.6$. Data are collected after 10^5 MCS.

cutters and the fractions of CLs or ILs have to be distinguished in each community. Similarly, the rates at which a node adds or cuts a link are different in each community. As a result, the general asymmetric case $m \neq 0$ turns out to be surprisingly complex, and its thorough analysis is presented elsewhere [74]. Here, our main goal is to present the salient features of the model in this general case and to highlight an original phenomenon, referred to as the “overwhelming transition,” occurring here under sufficient heterophily. We also provide arguments explaining the original phenomenology and provide some insights on how to generalize the analysis carried out in the symmetric case $m = 0$. For this, we first discuss the fraction of adders and CLs and then the degree distribution.

A. Fractions of adders and cross-links

We denote by α_σ the fraction of adders in the communities of opinion $\sigma = \pm$. Similarly, we denote by $\rho_\sigma = L_\times / (L_\times + 2L_{\sigma\sigma})$ the fraction of CLs in opinion group σ , giving the probability of a link connected to a node with opinion σ being a CL.

As a result of the asymmetry, in general $\alpha_+ \neq \alpha_-$ and $\rho_+ \neq \rho_-$, with $\alpha_\pm = \alpha$ and $\rho_\pm = \rho$ when $m = 0$. Hence, when $m \neq 0$, each panel of the counterpart of Fig. 3 contains twice as many curves, one for each community, as we see in Fig. 6 [to be compared with Fig. 3(a)]. The special case $J = 0$ is intuitively simple since the system thus behaves as if there was just a single population (the distinction of opinion is merely nominal), so that the addition and removal of links are unbiased. Hence, $\alpha_\pm = 1/2$ regardless of m . Furthermore, for an agent of opinion σ , the average fraction of CLs when $J = 0$ is simply the fraction of agents of the opposite opinion, yielding $\rho_\pm = n_\mp = (1 \mp m)/2$.

Simulation results show that in general $\alpha_\pm(m, J)$ and $\rho_\pm(m, J)$ are nontrivial functions of J and m ; see Fig. 6, where we find that α_\pm have a complex dependence on J and a very different shape when $m = -0.2$ [Fig. 6(a)] and $m = -0.6$ [Fig. 6(b)].

When $J > 0$, there is always a finite fraction of adders in both communities ($\alpha_\pm > 0$), whereas when $J < 0$, the fraction of adders in the smaller group (α_+ in Fig. 6) vanishes when heterophily is too strong. In other words, when J is close enough to -1 , the minority consists only of cutters. When $J > 0$ and both communities are of comparable sizes ($|m| \ll 1$), we recover a scenario similar to the symmetric case, e.g., Fig. 6(a), with a fraction of cutters and adders in both groups are comparable. However, for larger asymmetry, the fraction

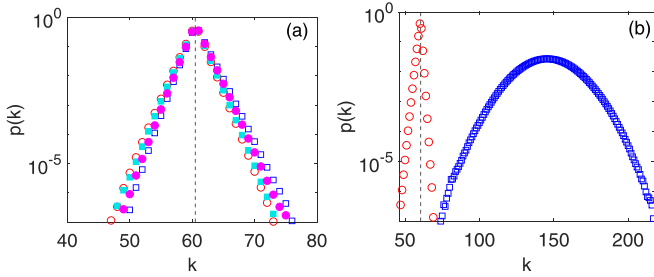


FIG. 7. Simulation results for the total degree distributions $p_{\pm}(k)$ in the community of ± 1 nodes for different values of J and m when $N = 1000$ and $\kappa = 60.5$. Data are collected after 10^5 MCS. Dashed lines are eyeguides showing $k = \kappa = 60.5$. (a) Symbols \square and \circ refer to p_+ and p_- , respectively, for $m = -0.2$, $J = -0.2$ (blue and red empty markers) and $J = 0.2$ (cyan and magenta filled markers). (b) Symbols \square (blue) \circ (red) refer respectively to p_+ and p_- , for $m = -0.6$, $J = -0.6$, when the minority agents are “overwhelmed” by those in the majority (see Sec. IV).

of adders in the smaller community is considerably larger than that in the majority agents [$\alpha_+ \gg \alpha_-$ in Fig. 6(b)] if $J > 0$, but otherwise ($\alpha_+ \ll \alpha_-$) for $J < 0$. Indeed, as noted above, α_+ is undetectably small when J drops below some threshold value (for example, when $m = -0.6$, the threshold is $J \approx -0.42$).

B. Total degree distribution and an “overwhelming” transition

Turning to degree distributions, we denote by $p_{\sigma}(k)$ the probability that an agent with opinion σ has k links in total (regardless of the opinion of its neighbors). Figure 7 clearly illustrates that $p_+(k) \neq p_-(k)$, with nontrivial dependence of $p_{\sigma}(k)$ on both m and J . In particular, in Fig. 7(b) with strong heterophily ($J = -0.6$), we notice that the minority community is characterized by degrees greatly exceeding κ and following a broad distribution.

For low asymmetry and small $|J|$, $p_{\sigma}(k)$ are qualitatively similar to the $p(k)$ above, compare Figs. 4(a) and 7(a) for $m = -0.2$ and $J = \pm 0.2$. Though $p_{\pm}(k)$ are no longer even functions of J , they are still (approximately) exponential distributions peaking near κ . Hence, the mean degree of all nodes is close to the preferred κ .

By contrast, striking behavior emerges under large asymmetry and high level of heterophily ($|m| = \mathcal{O}(1)$ and J near -1) as illustrated in Fig. 7(b) for $m = J = -0.6$. In this case, all minority agents are cutters, while the degree distribution (p_+ in Fig. 7) is *Gaussian-like*, with a mean much larger than κ . However, the distribution for a majority agent, $p_-(k)$ in Fig. 7, is comparable to those in the cases of small m , J : it is approximately an exponential distribution peaking around κ . Intuitively, this intriguing behavior stems from the combined effect of the preferred degree and heterophily mechanisms resulting in the minority agents being “overwhelmed” by those in the majority. In fact, when one group is larger than the other and strong heterophily favors the creation of CLs, agents in the smaller group can be “overwhelmed” by links created by members of the majority group, and their degree can exceed κ forcing them to act as cutters. By analogy with the mechanism of “homophily amplification” of Ref. [47] by which agents of

the same group interact and establish further connections, this phenomenon can thus be described as a sort of “heterophily amplification mechanism.”

To provide a more quantitative picture, we consider L_{\times} , the total number of CLs. Roughly, due to the large number of agents in the majority, these can act “as they wish” and settle with degrees around κ , which can provide an estimate for L_{\times} . If $J = 0$, then $\rho_- = n_+$, so that $L_{\times} = (\kappa N_-)n_+$. However, if heterophily is strong, then the most naive estimate of L_{\times} would be larger by a factor of $b = (1 - J)/(1 + J)$, which is the bias in favor of making CLs. Thus, a minority node (which has opinion $+$ here) would have $L_{\times}/N_+ \sim \kappa n_- b$ CLs. Thus, for large asymmetry and heterophily, the number of CLs alone can greatly exceed κ . Meanwhile, a minority agent is biased *against* cutting these CLs [suppressed by $(1 + J)/2$]. In this scenario, minority agents are overwhelmed by the majority adding links to them preferentially. Their cutting cannot keep up with the creation of links by the opposing group. As a result, their degrees are significantly larger than κ , as seen in Fig. 7(b). This is in striking contrast with what we have found in the symmetric case $m = 0$, where the degree distribution is always centered about κ , and shows that, when communities are of different sizes, simple update rules like those of the PDN can lead to a broad degree distribution with a large average degree of the smaller group. In Ref. [74], this picture is corroborated by a detailed analysis of the “overwhelming transition” and of $p_{\pm}(k)$ in terms of suitable analytical approximations. Interestingly, the authors of Ref. [44] studied a two-community growing network according to the preferential attachment dynamics with homophilic interactions, and showed that in their model heterophily helps increase the degree of the minority group, but these authors did not report the existence of an overwhelming transition in their model.

V. POLARIZATION

In this section, we study the phenomenon of polarization that measures the extent of division between communities with different opinions. We have seen that in the case of extreme homophily ($J = 1$), there is “fission”, which results in complete polarization with the network split into two separate communities; see Fig. 1(b). Oppositely, when there is extreme heterophily ($J = -1$), the network becomes bipartite, and in this case, there is complete antipolarization; see Fig. 1(e).

To characterize the level of partial division between the parties arising for intermediate homophily, $-1 < J < 1$ [Figs. 1(c) and 1(d)], polarization is often measured in terms of the so-called average edge homogeneity [36,72]. The latter quantity, here denoted by Λ , is defined as the difference between the fraction of ILs and CLs, that is $\Lambda = 1 - 2\rho$. When $m = 0$, it has a simple dependence on J that is well captured by Eq. (2), yielding $\Lambda = 2J/(1 + J^2)$. However, in general, the fractions of ILs and CLs, and hence Λ , depend on the size of each group (Nn_{\pm}) and on ρ_{\pm} . In the realm of the mean-field approximation, we indeed have $1/\rho_+ + 1/\rho_- = 2/\rho$, yielding

$$\Lambda = 1 - 2\rho = 1 - \frac{4\rho_+\rho_-}{\rho_+ + \rho_-}, \quad (8)$$

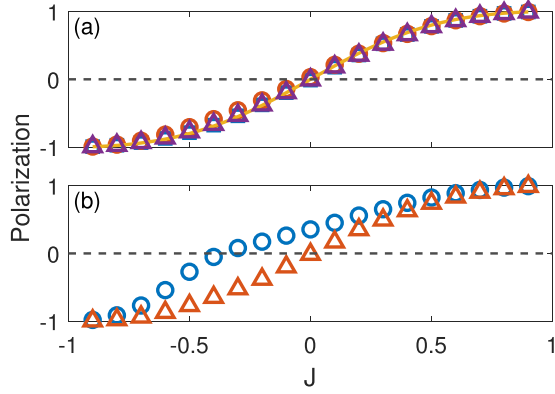


FIG. 8. Measures of polarization Λ and Π vs J for different values of m . Symbols are from simulation data. (a) $\Lambda = 1 - 2\rho$ for $m = 0$ (\square) and $m = -0.2$ (\circ), and Π for $m = -0.2$ (\triangle). The line shows the mean-field prediction $\Lambda = 2J/(1 + J^2)$ obtained for $m = 0$ by using Eq. (2) in Eq. (8), while Π has been computed from its definition Eq. (9) using simulation data. (b) Λ (\circ) and Π (\triangle) as functions of J with $m = -0.6$; when $J = 0$, $\Lambda = 0.36$ and $\Pi = 0$; see text. The dashed line is an eyeguide showing *zero* polarization. In all panels: $N = 100$ and $\kappa = 6.5$. Data are collected and sampled from 10^3 to 10^5 MCS.

which is a nontrivial function of m and J ; see Fig. 8. This quantity provides a meaningful measure of polarization in symmetric communities of similar sizes, i.e., when m is close to zero. In this case, Λ indeed captures the correct degree of polarization $\Lambda \rightarrow \pm 1$ when $J \rightarrow \pm 1$ and $\Lambda \propto J$ when $J \approx 0$; see Fig. 8(a). However, we note that Λ can provide misleading impressions for $m \neq 0$. This can be seen by noticing that when $J = 0$, $\rho_{\pm} = (1 \mp m)/2$, and Eq. (8) thus gives $\Lambda = m^2$, as in Fig. 8(b). However, when $J = 0$, agents not discriminating between the communities, there is no reason to associate it with any level of polarization: a proper measure of polarization under $J = 0$ should thus give zero.

For a better measure of polarization, we turn to the *joint* degree distribution $P_{\sigma}(\ell_{+}, \ell_{-})$. This quantity gives the probability that a node holding opinion σ has ℓ_{τ} links to agents with opinion $\tau = \pm$. These distributions are illustrated in Fig. 9, where $P_{+}(\ell_{+}, \ell_{-})$ and $P_{-}(\ell_{+}, \ell_{-})$ are, respectively, displayed by dark and light dots, and where each cell is labeled by (ℓ_{+}, ℓ_{-}) , with the size of the dots being proportional to $P_{\sigma}(\ell_{+}, \ell_{-})$. The averages

$$(\bar{\ell}_{\pm})_{\sigma} \equiv \sum_{\ell_{\pm}} \ell_{\pm} P_{\sigma}$$

can be regarded as the “centers of mass” (CMs) of the distributions P_{σ} . Clearly, the two CMs will not coincide in general, as illustrated by \triangle and ∇ in Fig. 9 (where they have been obtained from simulation data). Nevertheless, it can be shown that they do coincide when $J = 0$, where the opinions of the nodes are irrelevant [74]. Thus, the separation between the two CMs can serve as a suitable measure of polarization. Specifically, we define a “normalized” distance between CMs and measure of polarization as

$$\Pi \equiv \frac{1}{2} \left\{ \frac{(\bar{\ell}_{+})_{+} - (\bar{\ell}_{+})_{-}}{(\bar{\ell}_{+})_{+} + (\bar{\ell}_{+})_{-}} + \frac{(\bar{\ell}_{-})_{-} - (\bar{\ell}_{-})_{+}}{(\bar{\ell}_{-})_{-} + (\bar{\ell}_{-})_{+}} \right\}. \quad (9)$$

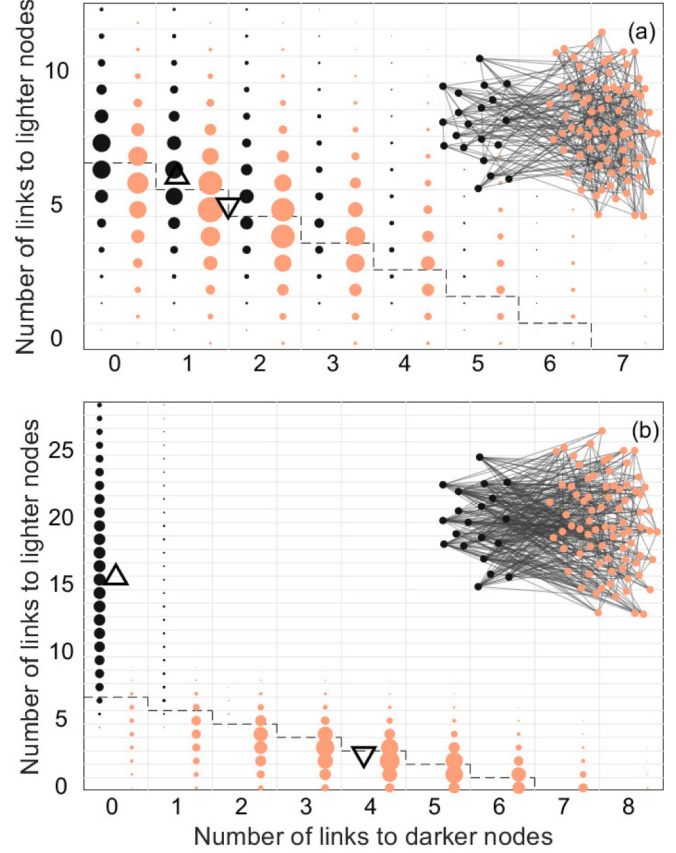


FIG. 9. Visualization of the joint degree distributions $P_{+}(\ell_{+}, \ell_{-})$ (dark dots) and $P_{-}(\ell_{+}, \ell_{-})$ (light dots) with $N = 100$, $\kappa = 6.5$ and $m = -0.6$. (a) $J = -0.1$; (b) $J = -0.6$: each dot represent a node holding opinion $+1$ (dark) or -1 (light). A node located in cell (ℓ_{+}, ℓ_{-}) has ℓ_{+} and ℓ_{-} links to $+1$ and -1 nodes, respectively, and total degree $\ell_{+} + \ell_{-} = k$. The area of each dark or light dot is proportional to the number of nodes having respectively ℓ_{+} and ℓ_{-} links to $+1$ and -1 nodes. Dashed lines show $\ell_{+} + \ell_{-} = \kappa$. \triangle and ∇ show, respectively, the centers of mass $(\bar{\ell}_{+}, \bar{\ell}_{-})_{\sigma}$ of nodes with opinion σ [e.g., \triangle is the center of mass of $P_{+}(\ell_{+}, \ell_{-})$]; see text. Data are collected and sampled from 10^3 to 10^5 MCS. Insets: illustration of typical network configurations after 1000 MCS.

In the case of complete polarization, there are no CLs, so $(\bar{\ell}_{\sigma})_{-\sigma}$ vanishes and $\Pi = 1$. Similarly, for antipolarization, there are no ILs, so $(\bar{\ell}_{\sigma})_{\sigma}$ vanishes and $\Pi = -1$. Furthermore, since $(\bar{\ell}_{\sigma})_{\sigma} = (\bar{\ell}_{\sigma})_{-\sigma}$ we have $\Pi = 0$ when $J = 0$ for all m . In other words, this definition of polarization vanishes in the absence of homophily for any asymmetry in the population sizes, and avoids the deficiencies of Λ . The quantity Eq. (9) has therefore the required properties to meaningfully characterize polarization in networks with communities of arbitrary sizes.

Figure 8 illustrates the salient features of Π with simulation results. We find that when $|m| \ll 1$, both Λ and Π are well approximated by $\Lambda \approx \Pi \approx 2J/(1 + J^2)$, where we have used the mean-field expression Eq. (2) for ρ in Eq. (8). With $m = -0.2$, Fig. 8(a) illustrates this property. However, for larger $|m|$, Π deviates from Λ for most values of J , as the data for $m = -0.6$ show in Fig. 8(b). To emphasize the advantage of Π over Λ as a measure of polarization, we

note that there is a regime when Λ remains positive even for heterophilic systems ($J < 0$)! By contrast, the sign of Π alone indicates which type of bias the agents have. We chose the parameters $(m, J) = (-0.6, -0.1)$ in the run for Fig. 9(a), for which numerically estimated $(\Lambda, \Pi) \approx (0.28, -0.10)$, to highlight this difference: while $\Lambda \approx 0.28$ implies the system is polarized, $\Pi \approx -0.10$ and the typical configuration clearly indicates antipolarization [see inset of Fig. 9(a)]. Comparing the values for Π in Fig. 8, we note that the overall dependence on m is relatively modest, which we interpret as an indication of the robustness of this measure. In other words, being mostly free from the influence from asymmetric community sizes, Π is indeed a better indicator of the effects of homophily on polarization. In Ref. [74], this analysis is corroborated by mean-field results allowing us to accurately reproduce the properties of Λ and Π for arbitrary m and J .

In Fig. 9(b), we illustrate the polarization and joint degree distribution under high heterogeneity and large asymmetry, $(m, J) = (-0.6, -0.6)$, in which case we have computed $(\Lambda, \Pi) \approx (-0.55, -0.87)$, corresponding to a high level of antipolarization. As discussed above, in the case of large asymmetry and high level of heterophily, the minority agents are “overwhelmed” by the majority, and their degree distribution is Gaussian-like with a mean much larger than κ ; see Fig. 7(b). This phenomenon is also clearly noticeable in Fig. 9(b), where P_+ differs greatly from P_- and from the joint distributions of Fig. 9(a), and nearly all minority agents have CLs and a degree exceeding κ . The comparison of Figs. 7(b) and 9(b) gives an insight into finite-size effects: while all the minority agents are cutters and there are no ILs within the minority community when $(N, \kappa) = (1000, 60.5)$ [see also Fig. 6(b)], a small number of minority agents are cutters and have a few ILs when $(N, \kappa) = (100, 6.5)$.

VI. DISCUSSION AND CONCLUSION

We have considered the dynamics of an out-of-equilibrium two-party network evolution model where agents hold fixed opinions and form dynamical links. These try to satisfy a preferred degree by endlessly creating and deleting edges. We have introduced homophily, a form of social interaction, to the simple preferred degree network dynamics. Unlike most network models with homophily [42,44], here the update rules are evolutionary, and homophily (or heterophily) influences the rate at which edges are created and removed.

Here, we have studied in detail systems where the parties are of the same size using both simulation techniques and mean-field theories. The excellent agreement between the analytical predictions and simulation results shows that we understand how the varying level of homophily shapes the degree distribution, the number of links across communities, and the level of polarization. These can help understand the phenomenon of filter bubbles [31] and echo chambers [32,33,35–37], especially when the level of polarization is high, which corresponds to the network where both parties have equally high levels of the fraction of internal links (influence assortment) [75], resulting in self-constructed echo chambers there.

Our model, under extreme homophily, exhibits complete fission of the population into two disconnected and polarized communities, previously found in models with rewiring

[54,55,57]. We have also introduced an original measure of polarization that does not share the counterintuitive properties associated with the average edge homogeneity, commonly used in the literature, and depends weakly on the community sizes.

Simulation results, corroborated by the detailed analysis of Ref. [74], show that our model exhibits a rich set of behavior when communities are of different sizes, especially when moderate to high levels of heterophily are present. In particular, a striking feature of this model is the existence of an “overwhelming transition”: under sufficient heterophily, agents in the smaller group are “overwhelmed” by links created by members of the majority group and only try to delete edges, and their degree distribution is Gaussian-like with an average much greater than the preferred degree. This transition therefore differs from fragmentation or fission [52,55,57] and transition to paradise [49] found in other network models with homophily. Our dynamic network model shaped by homophily therefore appears to be generally homogeneous with total degree distribution centered about the preferred degree, at the remarkable exception of the agents’ minority group that have a broad distribution and large degrees in the overwhelming phase.

The overwhelming transition is here attributed to the joint effect of heterophily and the existence of preferred degree. It would hence be interesting to investigate whether these two ingredients are sufficient to lead to a similar transition in other models, like those of Refs. [42,44,47], and whether the overwhelming transition is a generic feature of network models with homophily and a form of degree preference (not necessarily a strict degree value as here). It is also intriguing to notice that the increase of the degree of the minority group under sufficient heterophily, a salient feature of our model that is related to the overwhelming transition, has also been found in a two-community network growing according to the preferential attachment dynamics where it originates from a different mechanism [44]. Just as rewiring schemes [56] can be naturally extended to co-evolutionary models, where network varies in response to changes of node states and these change in response to updates of the network links [52,54,55,57,58,76–78], our model can be generalized to include coupled node and link coevolutionary dynamics. We expect that the phenomenology of such a co-evolutionary dynamics of a preferred degree network with homophily will lead to an even richer and more complex phenomenology, to understand which this study is certainly a necessary building block.

ACKNOWLEDGMENTS

We thank Andrew Mellor for substantive input, as well as Kevin Bassler and Henk Hilhorst for helpful discussions. The support of a joint Ph.D. studentship of the Chinese Scholarship Council and University of Leeds to X.L. is gratefully acknowledged (Grant No. 201803170212). We are also grateful to the London Mathematical Society (Grant No. 41712) and Leeds School of Mathematics for their financial support, and R.K.P.Z. is thankful to the Leeds School of Mathematics for their hospitality at an early stage of this collaboration.

- [1] T. C. Schelling, *Micromotives and Macrobehavior* (WW Norton and Company, New York, 1978).
- [2] C. Castellano, S. Fortunato, and V. Loreto, *Rev. Mod. Phys.* **81**, 591 (2009).
- [3] S. Galam, *Sociophysics: A Physicist's Modeling of Psychopolitical Phenomena* (Springer Science and Business Media, New York, 2012).
- [4] P. Sen and B. K. Chakrabarti, *Sociophysics: An Introduction* (Oxford University Press, Oxford, 2013).
- [5] A. Jedrzejewski and K. Sznajd-Weron, *C. R. Physique* **20**, 244 (2019).
- [6] R. Albert and L. Barabási, *Rev. Mod. Phys.* **74**, 47 (2002).
- [7] S. N. Dorogovtsev and J. F. F. Mendes, *Evolution of Networks: From Biological Nets to the Internet and WWW* (Oxford University Press, Oxford, 2003).
- [8] M. Newman, *Networks* (Oxford University Press, Oxford, 2010).
- [9] G. Szabo and G. Fáth, *Phys. Rep.* **446**, 97 (2007).
- [10] T. Antal, S. Redner, and V. Sood, *Phys. Rev. Lett.* **96**, 188104 (2006).
- [11] V. Sood, T. Antal, and S. Redner, *Phys. Rev. E* **77**, 041121 (2008).
- [12] G. J. Baxter, R. A. Blythe, and A. J. McKane, *Phys. Rev. Lett.* **101**, 258701 (2008).
- [13] R. A. Blythe, *J. Phys. A: Math. Theor.* **43**, 385003 (2010).
- [14] C. Castellano, M. Marsili, and A. Vespignani, *Phys. Rev. Lett.* **85**, 3536 (2000).
- [15] P. Moretti, S. Liu, C. Castellano, and R. Pastor-Satorras, *J. Stat. Phys.* **151**, 113 (2013).
- [16] A. Szolnoki, M. Perc, and M. Mobilia, *Phys. Rev. E* **89**, 042802 (2014).
- [17] D. Sabsovich, M. Mobilia, and M. Assaf, *J. Stat. Mech.: Theory Exp.* **2017**, 053405.
- [18] M. E. J. Newman, *Phys. Rev. E* **67**, 026126 (2003).
- [19] M. Boguná, R. Pastor-Satorras, A. Diaz-Guilera, and A. Arenas, *Phys. Rev. E* **70**, 056122 (2004).
- [20] Y. Murase, H.-H. Jo, J. Török, J. Kertész, and K. Kaski, *Sci. Rep.* **9**, 4310 (2019).
- [21] M. McPherson, L. Smith-Lovin, and J. M. Cook, *Ann. Rev. Sociol.* **27**, 415 (2001).
- [22] D. Centola, *Science* **334**, 1269 (2011).
- [23] D. Centola and M. Macy, *Am. J. Sociol.* **113**, 702 (2007).
- [24] M. Del Vicario, A. Scala, G. Caldarelli, H. E. Stanley, and W. Quattrociocchi, *Sci. Rep.* **7**, 40391 (2017).
- [25] D. Centola, J. C. Gonzalez-Avella, V. M. Eguiluz, and M. S. Miguel, *J. Confl. Resolut.* **51**, 905 (2007).
- [26] Y. Volkovich, D. Laniado, K. E. Kappler, and A. Kaltenbrunner, in *Proceedings of the International Conference on Social Informatics* (Springer, Berlin, 2014), pp. 139–150.
- [27] D. Zeltzer, *Am. Econ. J.: Appl. Econ.* **12**, 169 (2020).
- [28] J. M. McPherson and L. Smith-Lovin, *Am. Sociol. Rev.* **52**, 370 (1987).
- [29] M. Yavaş and G. Yücel, *Soc. Sci. Comput. Rev.* **32**, 354 (2014).
- [30] C. R. Shalizi and A. C. Thomas, *Sociol. Method Res.* **40**, 211 (2011).
- [31] E. Pariser, *The filter bubble: What the Internet is Hiding from You* (Penguin, London, 2011).
- [32] S. Iyengar, G. Sood, and Y. Lelkes, *Public Opin. Q.* **76**, 405 (2012).
- [33] P. Barberá, J. T. Jost, J. Nagler, J. A. Tucker, and R. Bonneau, *Psychol. Sci.* **26**, 1531 (2015).
- [34] P. Barberá, *Polit. Anal.* **23**, 76 (2015).
- [35] E. Bakshy, S. Messing, and L. A. Adamic, *Science* **348**, 1130 (2015).
- [36] M. Del Vicario, A. Bessi, F. Zollo, F. Petroni, A. Scala, G. Caldarelli, H. E. Stanley, and W. Quattrociocchi, *Proc. Natl. Acad. Sci. USA* **113**, 554 (2016).
- [37] X. Wang, A. D. Sirianni, S. Tang, Z. Zheng, and F. Fu, *Phys. Rev. X* **10**, 041042 (2020).
- [38] W. Xie, M.-X. Li, Z.-Q. Jiang, Q.-Z. Tan, B. Podobnik, W.-X. Zhou, and H. E. Stanley, *Sci. Rep.* **6**, 18727 (2016).
- [39] P. Ramazi, J. Riehl, and C. M., *R. Soc. Open Sci.* **5**, 180027 (2018).
- [40] O. Barranco, C. Lozares, and D. Muntanyola-Saura, *Qual. Quant.* **53**, 599 (2019).
- [41] M. Yokomatsu and H. Kotani, *J. Math. Sociol.* **45**, 111 (2021).
- [42] F. Gargiulo and Y. Gandica, *J. Artif. Soc. Soc. Simul.* **20**, 8 (2017).
- [43] L. H. Wong, P. Pattison, and G. Robins, *Physica A* **360**, 99 (2006).
- [44] F. Karimi, M. Génois, C. Wagner, P. Singer, and M. Strohmaier, *Sci. Rep.* **8**, 11077 (2018).
- [45] D. Kimura and Y. Hayakawa, *Phys. Rev. E* **78**, 016103 (2008).
- [46] F. Papadopoulos, M. Kitsak, M. Á. Serrano, M. Boguná, and D. Krioukov, *Nature (London)* **489**, 537 (2012).
- [47] A. Asikainen, G. Iñiguez, J. Ureña-Carrión, K. Kaski, and M. Kivelä, *Sci. Adv.* **6**, eaax7310 (2020).
- [48] P. L. Krapivsky and S. Redner, *Phys. Rev. E* **103**, L060301 (2021).
- [49] P. J. Gorski, K. Bochenina, J. A. Holyst, and R. M. D'Souza, *Phys. Rev. Lett.* **125**, 078302 (2020).
- [50] J. Overgoor, A. Benson, and J. Ugander, in *Proceedings of the World Wide Web Conference (ACM, New York, 2019)*, pp. 1409–1420.
- [51] F. Heider, *The Psychology of Interpersonal Relations* (Psychology Press, Hove, 1958).
- [52] P. Holme and M. E. J. Newman, *Phys. Rev. E* **74**, 056108 (2006).
- [53] T. Evans, *Eur. Phys. J. B* **56**, 65 (2007).
- [54] F. Vazquez and V. M. Eguiluz, *New J. Phys.* **10**, 063011 (2008).
- [55] F. Vazquez, V. M. Eguiluz, and M. S. Miguel, *Phys. Rev. Lett.* **100**, 108702 (2008).
- [56] J. Lindquist, J. Ma, P. Van den Driessche, and F. H. Willeboordse, *Physica D* **238**, 370 (2009).
- [57] R. Durrett, J. P. Gleeson, A. L. Lloyd, P. J. Mucha, F. Shi, D. Sivakoff, J. E. S. Socolar, and C. Varghese, *Proc. Natl. Acad. Sci. USA* **109**, 3682 (2012).
- [58] A. D. Henry, P. Prafat, and C. Zhang, *Proc. Natl. Acad. Sci. USA* **108**, 8605 (2011).
- [59] M. Mobilia, *Phys. Rev. E* **92**, 012803 (2015).
- [60] C. Castellano, M. A. Muñoz, and R. Pastor-Satorras, *Phys. Rev. E* **80**, 041129 (2009).
- [61] A. Mellor, M. Mobilia, and R. K. P. Zia, *Phys. Rev. E* **95**, 012104 (2017).
- [62] M. Mobilia, A. Petersen, and S. Redner, *J. Stat. Mech.* (2007) P08029.
- [63] W. Liu, S. Jolad, B. Schmittmann, and R. K. P. Zia, *J. Stat. Mech.* (2013) P08001.

- [64] W. Liu, B. Schmittmann, and R. K. P. Zia, *J. Stat. Mech.* (2014), [P05021](#).
- [65] K. E. Bassler, D. Dhar, and R. K. P. Zia, *J. Stat. Mech.* (2015) [P07013](#).
- [66] M. Mobilia, *J. Stat. Phys.* **151**, 69 (2013).
- [67] M. Mobilia, *Phys. Rev. Lett.* **91**, 028701 (2003).
- [68] S. Galam and F. Jacobs, *Physica A* **381**, 366 (2007).
- [69] K. Sznajd-Weron, M. Tabiszewski, and A. M. Timpanaro, *Europhys. Lett.* **96**, 48002 (2011).
- [70] D. Acemoglu, G. Como, F. Fagnani, and A. Ozdagla, *Math. Oper. Res.* **38**, 1 (2013).
- [71] W. Liu, B. Schmittmann, and R. K. P. Zia, *Europhys. Lett.* **100**, 66007 (2012).
- [72] H. A. Prasetya and T. Murata, *Comput. Soc. Netw.* **7**, 2 (2020).
- [73] P. Erdős and A. Rényi, *Publicationes Mathematicae Debrecen* **6**, 290 (1959).
- [74] X. Li, M. Mobilia, A. M. Rucklidge, and R. K. P. Zia, [arXiv:2107.13945](#).
- [75] A. J. Stewart, M. Mosleh, M. Diakonova, A. A. Arechar, D. G. Rand, and J. B. Plotkin, *Nature (London)* **573**, 117 (2019).
- [76] C. Nardini, B. Kozma, and A. Barrat, *Phys. Rev. Lett.* **100**, 158701 (2008).
- [77] G. Iniguez, J. Kertész, K. K. Kaski, and R. A. Barrio, *Phys. Rev. E* **80**, 066119 (2009).
- [78] T. Gross and B. Blasius, *J. R. Soc. Interface* **5**, 259 (2008).